

Heat Transfer Enhancement Using Augmented Tubes for Desalination Using Fuzzy-TOPSIS Approach

R. Kaushal¹, R. Kumar²

1. Department of Mechanical Engineering, National Institute of Technology, Kurukshetra, Haryana 136119, India
2. Department of Mechanical Engineering, Lovely Professional University, Phagwara, Punjab 144411, India.

Receive Date 23 September 2019; Revised 11 October 2019; Accepted Date 20 October 2019

*Corresponding author: rav.chauhan@yahoo.co.in (R. Kumar)

Abstract

This paper deals with the falling film heat transfer across horizontal copper tubes at different tube surface geometries, mass flow rates, heat fluxes, and weight percentage of salt in water salt solutions at the atmospheric pressure. The falling film heat transfer coefficient is significantly affected by the heat flux, film Reynolds number, and water salt solutions for the three types of augmented tubes viz. spiral, splined, and smooth. This paper considers the influence of the operating parameters on the heat transfer coefficient using the Fuzzy-TOPSIS applications. The experimental results obtained reveal that the falling film heat transfer is greatly enhanced in case of the spiral tube when compared with the splined and smooth tubes. The spiral tube shows a significant heat transfer performance than the other two tubes for a given heat flux, and Reynolds number as the heat flux increases the surface temperature, and also increases and increment in the surface temperature of the smooth tube is greater than the spiral and spline tubes for a given heat flux and Reynolds number. As the mass flow rate increases, the surface temperature of all the three tubes decreases but for a given heat flux and Reynolds number, the smooth tube has a more surface temperature than the other two tubes.

Keywords: *Falling film, Heat exchanger, Enhanced tubes, Fuzzy-TOPSIS applications.*

1. Introduction

Falling film horizontal tube heat exchangers are utilized in various processing industries. This type of heat exchangers has been studied over the years in terms of the effects such as the liquid tube spacing and heat flux. Gorgy et al. [1] have tested various combinations of refrigerants and tubes, concluding that the heat transfer coefficient increases with increase in the heat flux for all cases. Habert et al. [2] have concluded the pool boiling performance of the different tubes, and showed similar results as the literature in terms of the heat transfer coefficient. Moeykens et al. [3] have concluded that the enhanced surface provides higher results than the finned tubes but lower performances than the enhanced condensing surfaces used for evaporation. It has also been concluded that an increase in the heat transfer coefficient takes place with heat flux up to a specific value, after which, the heat transfer coefficient starts decreasing with increase in the heat flux. This is probably due to the partial dry-out. Chien and Webb et al. [4] have tested and enhanced a tube similar to Turbo-B using R-11 and R-123. It was concluded that at a low heat flux, the tube that had smaller total open areas resulted in a

higher heat transfer coefficient. On the other side, at higher heat fluxes, the tube that had larger total open areas gave a higher heat transfer coefficient. Fujita and Tsutsui et al. [5, 6] defined two flow modes as follow: a distinct droplet mode and a disturbed jet mode. It has been noted that the transition between the droplets and the jet mode occurs at the Reynolds number around 100 independent feeding methods. Hu et al. [7] have suggested the following flow modes: the droplet mode, droplet jet mode, an unsteady jet mode-characterized by a steadiness in the location of the jet departure site-the inline jet mode, staggered jet mode, jet-sheet mode, and sheet mode. Liu and Yi et al. [8] have suggested the convective and the boiling regimes for the falling films. In the convective regime, as the boiling regime, the heat transfer coefficient increases with the heat flux. It was suggested that both regimes were independent from the surface configuration. Wang et al. [9], using the boiling-enhanced surfaces, and Zeng et al. [10], using the finned and corrugated surfaces, observed the boiling regime only. On the other hand, Kuwahara et al. [11] have pointed out a marginal effect of heat flux on a boiling enhanced

surface despite the occurrence of the bubble nucleation. In this experiment, a spline and spiral groove tube was used as a new type of enhanced heat transfer tube. The working process for the tube was performed simply by using a lathe machine, and hence was of low cost compared with various commercial enhanced tubes. Maddah et al. [33] have suggested a factorial experimental design for a double pipe heat exchanger to improve the thermal performance.

This study initially evoked the heat transfer of water and water-salt solution falling film on the smooth, spline, and spiral grooved tubes. The experimental outcomes depict that the spiral tube is a suitable efficient heat transfer tube for the convective heat transfer for both the water-salt and water solution in comparison with the spline and smooth tubes. At a constant heat flux, as the Reynolds number increases, heat transfer also increases for all the three tubes. In this context, the critical parameters were identified on which the heat transfer coefficients were mostly dependent. Such problems can be easily solved using the multiple attribute decision-making (MADM) approach [12]. Under these methodologies and due to their novel application domains, many works have been reported [13-17]. Numerous methods have been reported under the MADM category. These include simple additive weighting (SAW), analytic hierarchy process (AHP) [18], graph theory and matrix approach (GTMA) [19], polygons area method [20], technique for order preference by similarity to ideal solution (TOPSIS) [21], and many others. Among all these, TOPSIS and VIKOR are outstanding MADM approaches, which have been designed to face with rational and irrational decision-making [22]. It has been applied to various problems ranging from evaluating supplier selection strategy [23, 24, 26], group decision-making [29], machine tool selection [27], material selection [25], and performance evaluation [28]. In the present work, we employed the fuzzy TOPSIS approach to evaluate the performance parameters and rank the rival dependent on the heat transfer coefficient. Four parameters have been applied for evaluation of the

performance of heat transfer coefficient for the different shape tubes. The various parameters involved are Reynolds number (P1), heat flux (P2), feeder height (P3), salt content (P4), and tube surface design. The present work underlines assessing the efficiency of heat transfer coefficient with various parameters utilizing TOPSIS. This is achieved by first computing the parameters utilizing fuzzy, and after that utilizing the TOPSIS strategies to summarize the outcome. The artificial intelligent techniques are also in use to improve the thermal performance of the system [34].

1.1. Fuzzy Logic

Fuzzy deals with the issues where it is difficult to recognize between the member and non-member objects of a problem. Fuzzy logic is based on a set theory. It consists of a membership function within the interval [0,1], which describes the extent of relevance of an element for being the member of the set. Linguistic variables are used for all the comparisons, which are assigned numerical values without any enigma. A linguistic variable is a variable whose value are words or sentences in a natural or artificial language. The major advantage of the linguistic approach locates in the realm of humanistic system, especially in the fields of linguistics, human decision processes, psychology, artificial intelligence, economics, and related areas. Different fuzzy numbers are used depending on their situation. In the present work, we used the trapezoidal fuzzy numbers (b_1, b_2, b_3, b_4) for $\{b_1, b_2, b_3, b_4 \in R; b_1 \leq b_2 \leq b_3 \leq b_4\}$; as

shown in figure 1. The membership function $\mu^b(x)$ of trapezoidal fuzzy number is defined as:

$$\mu_b(x) = \begin{cases} \frac{x-b_1}{b_2-b_1}, & x \in [b_1, b_2] \\ 1, & x \in [b_2, b_3] \\ \frac{b_4-x}{b_4-b_3}, & x \in [b_3, b_4] \\ 0, & \text{otherwise} \end{cases} \quad (1)$$



Figure 1. Trapezoidal fuzzy number.

1.2. TOPSIS Method

TOPSIS is a method used to solve the MADM problem from a finite set of alternatives [30]. It implies that a decision matrix having “p” types of tubes and “q” attributes can be thought to be an issue of “q” dimensional hyper plane having “p” points whose area is given by the estimation of their attributes. The essential principle is that the picked alternatives have the least distance from the positive ideal solution (best case arrangement) and the farthest ways from the negative ideal solution (most pessimistic scenario arrangement). The ideal solution is an answer that expands the advantage qualities and limits the cost traits, though the negative ideal solutions increase the cost properties and limit the advantage characteristics [31, 32]. The various procedures involved in the calculation of TOPSIS index are as follow:

Step 1: Normalize the matrix as given below:

$$r_{ij} = \frac{f_{ij}}{\sqrt{\sum_{i=1}^m (f_{ij})^2}}; \quad \forall j \quad (2)$$

Step 2: Calculate the weighted normalized decision matrix as given:

$$V_{ij} = [r_{ij}]_{p \times q} \times [W_j]_{q \times p}^{diagonal} \quad (3)$$

Step 3: Calculate the positive ideal and negative ideal solution:

The positive ideal solution V_j^+ and negative ideal solution V_j^- are as given below:

$$V_j^+ = \{(\max V_{ij}, j \in J_1), (\min V_{ij}, j \in J_2), i=1,2,3,\dots,p\}; \quad \forall j \quad (4)$$

$$V_j^- = \{(\min V_{ij}, j \in J_1), (\max V_{ij}, j \in J_2), i=1,2,3,\dots,p\}; \quad \forall j \quad (5)$$

where J_1 and J_2 represent the higher best and lower best criteria, respectively.

Step 4: Calculate the distance d_i^+ and d_i^- from the positive ideal solution and negative ideal solution, respectively.

$$d_i^+ = \left[\sum_{j=1}^q (V_{ij} - V_j^+)^2 \right]^{0.5}, \quad i=1,2,3,\dots,p \quad (6)$$

$$d_i^- = \left[\sum_{j=1}^q (V_{ij} - V_j^-)^2 \right]^{0.5}, \quad i=1,2,3,\dots,p \quad (7)$$

Step 5: Calculate the rank index as:

$$C_i^+ = \frac{d_i^-}{d_i^- + d_i^+} \quad (8)$$

Reasons of breakdown with highest rank index C_i^+ are preferred.

2. Experimental set-up

Figure 2 shows a schematic view of the experimental apparatus used in this work. It consists of a liquid circulation system, a pump, a liquid feeder, two enhanced tubes (i.e. spline and helical grooved) in a test section, a flow-meter, a digital temperature indicator, a digital voltmeter, and a digital ammeter. The working fluid is pumped up from the reservoir to the feeder through the flowmeter and regulating valves that maintain the film Reynolds number. Here, the fluid will be heated to a certain temperature by the heater placed in the reservoir, and then it passes through a pump and a flow-meter, and then flows into the liquid feeder from which the fluid is supplied at the desired flow rate in the form of sheets flow pattern to the heated tube. Finally, it is flowed back into the reservoir to be recycled. The distance between the feeder and the horizontal heated tube is 24 mm.

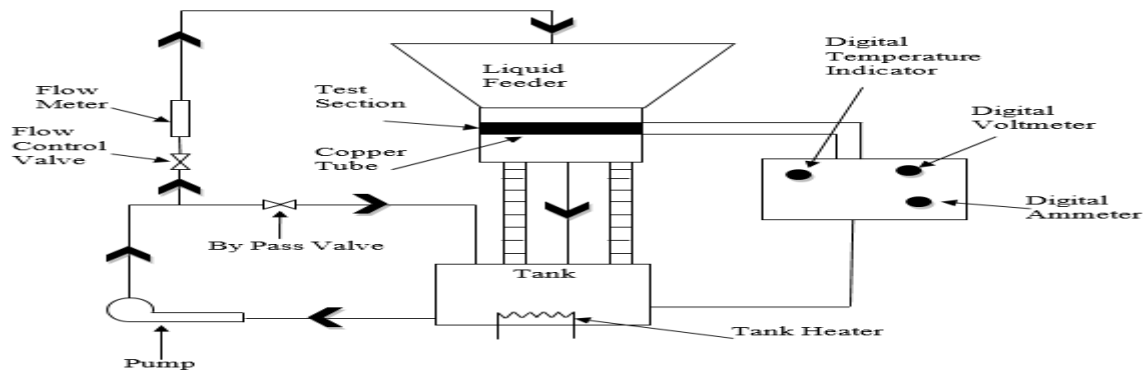


Figure 2. Line diagram of experimental set-up.

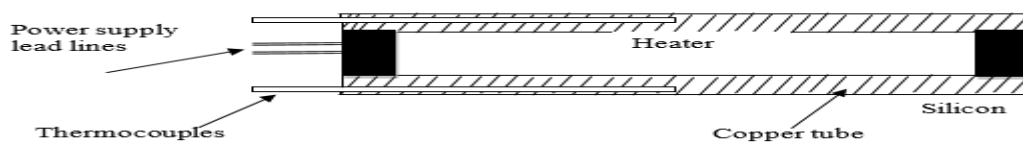


Figure 3. Inner structure of test tube.

The experimental conditions are represented in table 1.

Table 1. Experimental Condition.

Test liquid	Water/salt solution
Pressure	100 KPa
Salt concentration	0-10 wt.%
Reynolds number	13460-22745
Heat Flux	9080 W m ⁻² -26520 W m ⁻²
Tube diameter	19 mm
Liquid feed height	24 mm
Nozzle width	1 mm

Figure 3 demonstrates an evaporation tube instrument with a heater inside and four thermocouples that have an external width of 0.1 mm. The smooth tubes utilized in this test were made of copper with an external diameter of 19 mm, an inward diameter of 12 mm, and a length of 120 mm (an effective length of 100 mm). The spline tubes used in this experiment were made of copper with an outer diameter of 19 mm, an inner diameter of 12 mm, a length of 120 mm (an effective length of 100 mm), and a width of 2 mm. Also 2 mm depth slots were cut throughout the outer periphery with a cross-section angle of 30° between the slots. The spiral tubes used in this experiment were made of copper with an outer diameter of 19 mm, an inner diameter of 12 mm,

and a length of 120 mm (an effective length of 100 mm) with a helix angle of 60° and a pitch of 0.6 mm. A heat flux was given by a heater 10 mm in measurement installed within the cylinder. Two thermocouples were put on the external surface of the tube. The average estimated temperatures at these areas were taken to be the tube wall temperatures. One thermocouple was set inside the water supply tank and utilized to characterize the heat transfer coefficients.

3. Results and Discussion

3.1 Tests for pure water

Figure 4 shows that as the Reynolds number increases, the heat transfer coefficient increases for a given heat flux but after a certain value it becomes constant and the sheet flow pattern becomes fully developed as the tube surface is totally covered by water film, and so there is no scope for a heat transfer enhancement. The spiral tube shows a more significant heat transfer performance than the other two tubes for a given heat flux and the Reynolds number because the spiral tube film breakdown does not occur. Also it has a more surface area than the smooth tube. Figure 5 shows that the heat flux affects the heat transfer coefficient significantly. As the heat flux increases, the heat transfer coefficient increases, and for all the three tubes, it is almost increased in the same manner. Figure 6 shows that as the heat flux increases, the surface temperature also increases and increment in the surface temperature of the smooth tube is greater than the spiral and spline tubes for a given heat flux and Reynolds number.

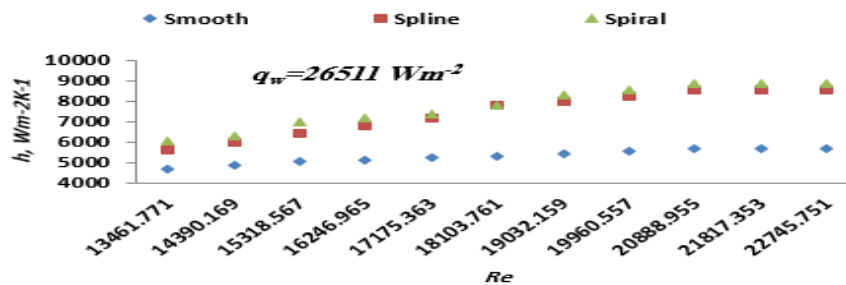


Figure 4. Comparison of the enhanced tube with the smooth tube for different Reynolds numbers.

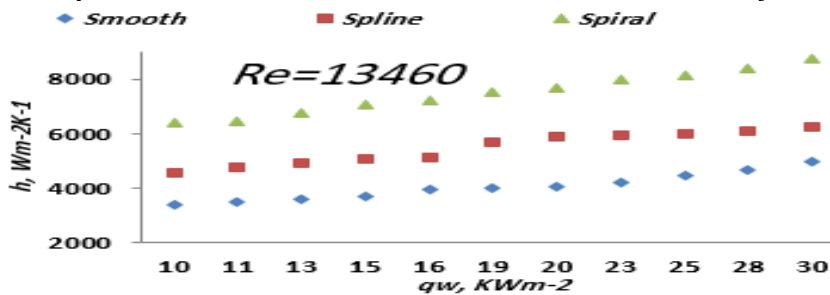


Figure 6. Effect of heat flux on the surface temperature of the smooth and enhanced tubes.

3.2 Tests for water salt solution

Figure 7 shows that a 10 wt.% salt solution has a poorer heat transfer performance than pure water at a given heat flux and Reynolds number for all the three tubes but increment in the heat transfer coefficient for a 10 wt.% salt solution is similar

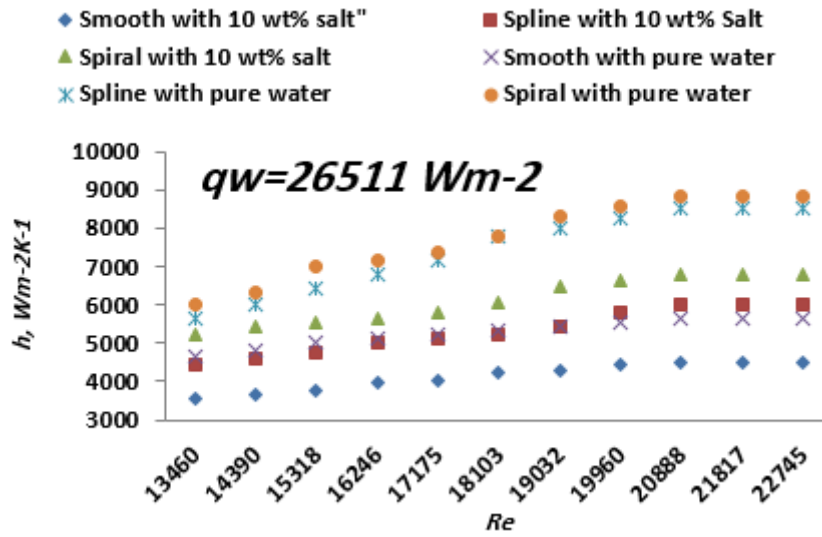


Figure 7. Comparison of the smooth and enhanced tubes for pure water and 10 wt% salt in water salt solution with different Reynolds numbers.

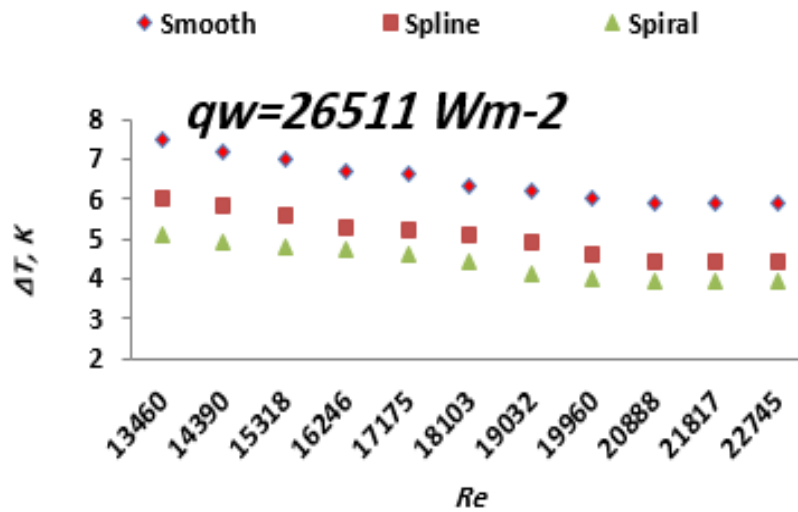


Figure 8. Effect of Reynolds number on the surface temperature of the smooth and enhanced tubes.

3.3 Correlation

The correlation for the heat transfer coefficient and heat flux with the Reynolds number, derived using the multiple regression analysis and their qualitative effects, were studied.

$$h = 2.95(q_w)^{.32}(Re)^{.43} \quad (9)$$

(for $13460 \leq Re \leq 22745$, $9080 \leq q_{flux} \leq 26520$)

The above correlation showed a good agreement between the experimental and predicted values of heat transfer coefficient with an error of $\pm 2\%$ for the smooth tube with pure water. This correlation

with pure water. Figure 8 shows that as the mass flow rate increases, the surface temperature of all the three tubes decreases but for a given heat flux and Reynolds number, the smooth tube has a more surface temperature than the other two tubes.

showed that the Reynolds number put a slightly more effect than the heat flux on the heat transfer coefficient.

$$H = .37(q_w)^{.25}(Re)^{.75} \quad (10)$$

(for $13460 \leq Re \leq 22745$, $9080 \leq q_{flux} \leq 26520$)

The above correlation showed a good agreement between the experimental and predicted values for the heat transfer coefficient with an error of $\pm 2\%$ for the spline tube with pure water. This correlation showed that the Reynolds number put a significant effect on the heat transfer coefficient rather than the heat flux.

$$h = 178.34(q_w)^{-12}(Re)^{27} \tag{11}$$

(for $13460 \leq Re \leq 22745$, $9080 \leq q_{flux} \leq 26520$)

The above correlation showed a good agreement between the experimental and predicted values for the heat transfer coefficient with an error of $\pm 6\%$ for the spiral tube with pure water. This correlation showed that the Reynolds number put a slightly more effect on the heat transfer coefficient than the heat flux.

$$h = 57.01(q_w)^{-05}(Re)^{49} \tag{12}$$

(for $13460 \leq Re \leq 22745$, $9080 \leq q_{flux} \leq 26520$)

The above correlation showed a good agreement between the experimental and predicted values for the heat transfer coefficient with an error of $\pm 1\%$ for the smooth tube with water salt solution. This correlation shows that as we increase the heat flux, the heat transfer coefficient decreases, while it increases with the Reynolds number under the above given range.

$$h = .52(q_w)^{16}(Re)^{77} \tag{13}$$

(for $13460 \leq Re \leq 22745$, $9080 \leq q_{flux} \leq 26520$)

The above correlation showed a good agreement between the experimental and predicted values for the heat transfer coefficient with an error of $\pm 2\%$ for the spline tube with water salt solution. This correlation showed that the Reynolds number put a significant effect on the heat transfer coefficient rather than the heat flux.

$$H = .18(q_w)^{29}(Re)^{76} \tag{14}$$

(for $13460 \leq Re \leq 22745$, $9080 \leq q_{flux} \leq 26520$)

The above correlation showed a good agreement between the experimental and predicted values for the heat transfer coefficient with an error of $\pm 3\%$ for the spline tube with water salt solution. This correlation showed that the Reynolds number put a significant effect on the heat transfer coefficient rather than the heat flux.

3.4 Factor ranking with FUZZY-TOPSIS

The subsequent stage was correlation for all cylinders for every standard. In this unique circumstance, the fluffy methodology was utilized as it functioned admirably where there was a need of speculative scale to incorporate the verbal thinking of different leaders. It utilizes the semantic factors for the examination of various cylinders.

Table 4. Calculated crisp values for assigned fuzzy rates of tubes.

Factors	Crisp values for smooth tube	Crisp values for spline tube	Crisp values for spiral tube	Rank indices	Ranking
Reynolds No.	0.925926	0.740741	0.592593	0.691281	1
Heat flux	0.833333	0.944444	0.366667	0.615249	2
Feeder height	0.407407	0.740741	0.925926	0.369007	4
Salt concentration	0.888889	0.611111	0.611111	0.610575	3

These were additionally changed over into fuzzy numbers utilizing table 2. A short time later, the fuzzy appraisals were collected, standardized, and defuzzified. Table 3 obliges the subjective verbal assessment of the chiefs filled by us (choice compilers) in the light of our discourse with different leaders.

Table 2. Linguistic variable with fuzzy number.

Linguistic variable	Fuzzy number
Very High (VH)	(0.8, 0.9, 1.0, 1.0)
High (H)	(0.7, 0.8, 0.8, 0.9)
Above Average (AA)	(0.5, 0.6, 0.7, 0.8)
Average (A)	(0.4, 0.5, 0.5, 0.6)
Below Average (BA)	(0.2, 0.3, 0.4, 0.5)
Low (L)	(0.1, 0.2, 0.2, 0.3)
Very Low (VL)	(0.0, 0.0, 0.1, 0.2)

Table 3. Linguistic decision matrix of tubes for all evaluation criteria.

Parameters	Smooth (C ₁)	Spline (C ₂)	Spiral (C ₃)
P ₁	VH	H	AA
P ₂	VH	EH	A
P ₃	A	H	VH
P ₄	AA	A	A

The best range is termed exceptionally high (EH), while the worst is termed extremely low (EL). Table 4 arguments the corresponding crisp values of the aggregated fuzzy ratings.

The crisp values thus obtained were used to calculate the priority vectors for each criterion with respect to different tubes. Table 5 shows the utility measures and rank indices for TOPSIS. We sum up

our study with a hope that such analysis can be proven extremely helpful for determining the factor affecting mostly on the film heat transfer coefficient.

Table 5. Rank indices from TOPSIS

Factors	Positive ideal solution (d ⁺)	Negative ideal solution (d ⁻)	Rank indices	Ranking
Reynolds No.	0.022951	0.051392	0.691281	1
Heat flux	0.029779	0.04762	0.615249	2
Feeder height	0.05149	0.030111	0.369007	4
Salt concentration	0.03015	0.047271	0.610575	3

4. Conclusion

A number of experiments were carried out on the heat transfer coefficients of the falling film horizontal heated tube, and it was observed that the heat transfer coefficient for the spiral tube was more than those for the other understudied tubes. As the Reynolds number increased, the heat transfer coefficient increased first and then remained constant for a given heat flux. The spiral tube showed a significant heat transfer performance than the other two tubes for a given heat flux and Reynolds number. With an increase in the heat flux, the heat transfer coefficient increased for all the understudied three tubes. As the heat flux increased, the surface temperature also increased, and the increment in the surface temperature of the smooth tube was greater than the spiral and spline tubes for a given heat flux and Reynolds number. As the Reynolds number increased, the temperature difference between the tube surface and the flowing liquid decreased. It was also concluded that the water salt solution heat transfer performance was poorer than pure water for all the three tubes. As the heat flux increased, the surface temperature of the tubes increased for pure water.

Nomenclature

- d Tube diameter, mm
- h Heat transfer coefficient ($h = q_w/\Delta T$), $W m^{-2} K^{-1}$
- q_w Average wall heat flux, $W m^{-2}$
- Re Film Reynolds number ($Re = 4\Gamma/\mu$)
- T_l Liquid temperature at the exit of feeder, K
- T_w Average wall temperature, K
- ΔT Temperature difference between tube surface and liquid ($\Delta T = T_w - T_l$)
- Γ Falling film mass flow rate per unit length on one side of tube, $kg m^{-1} s^{-1}$
- μ Dynamic viscosity, $kg m^{-2} s^{-1}$

References

- [1] Gorgy, E.I., 2008. Pool boiling of R-134a and R-123 On smooth and enhanced tubes. Master`s thesis. Kanass University, Department of Mechanical and Nuclear Engineering.
- [2] Habert, M., 2009. Falling Film Evaporation on a Tube Bundle with Plain and enhanced tubes. Ph.D. Thesis. Ecole Polytechnique Federale de Lausanne, Laboratory of Heat and Mass Transfer, Lausanne, Switzerland.
- [3] Moeykens, S.A., Huebsch, W.W., Pate, M.B., 1995. Heat transfer of R-134a in single tube spray evaporation including lubricant effect and enhanced surface results. ASHRAE Trans. 101, 111-123.
- [4] Chien, L.H., Webb, R.L., 1998a. A parametric study of nucleate boiling on structured surfaces, part 1: effect of tunnel dimensions. J. Heat Transfer 120, 1042-1048.
- [5] Y. Fujita, M. Tsutsui, Experimental and analytical study of evaporation heat transfer in falling films on horizontal tubes, Proceedings of the 10th international heat transfer conference, Brighton, vol. 6 1994, p. 175-80.
- [6] Y. Fujita, M. Tsutsui, Evaporation heat transfer of falling films on horizontal tube. Part 2. Experimental study, Heat Transfer –Jpn Res 24 (1995) 17-31.
- [7] X. Hu, A.M. Jacobi, The intertube falling film. Part 1. Flow characteristics, mode transitions, and hysteresis, J Heat Transfer 118 (1996) 616-625.
- [8] Z.H. Liu, J. Yi, Enhanced evaporation heat transfer of water and R-11 falling film with the roll-worked enhanced tube bundle, Exp Thermal Fluid Science 25 (2001) 447-455.
- [9] G. Wang, Y. Tan, S. Wang, N. Cui, A study of spray falling film boiling on horizontal mechanically made porous surface tubes, Proceedings of the international symposium of heat and mass transfer enhancement and energy conservation (ISHTEEC), Guangzhou, 1988, p. 425-32.
- [10] X. Zeng, M. C. Chyu, Z. H. Ayub, Ammonia spray evaporation heat transfer performance of single long-fin and corrugated tubes, ASHRAE Trans 104 (1A) (1998) 185-196.

- [11] H. Kuwahara, A. Yasukawa, W. Nakayama, T. Yanagida, Evaporative heat transfer from horizontal enhanced tubes in thin film flow, *Heat Transfer-Jpn Res* 19 (1990) 83-97.
- [12] Vats, Gaurav, and Rahul Vaish. Piezoelectric material selection for transducers under fuzzy environment. *Journal of Advanced Ceramics* 2.2 (2013): 141-148.
- [13] Vats, Gaurav, and Rahul Vaish. Phase Change Materials Selection for Latent Heat Thermal Energy Storage Systems (LHTESS): An Industrial Engineering Initiative Towards Materials Science. *Advanced Science Focus* 2.2 (2014): 140-147.
- [14] Vats, G., & Vaish, R. (2014b). Selection of Lead-Free Piezoelectric Ceramics. *International Journal of Applied Ceramic Technology*, 11(5): 883-893.
- [15] Vats, G., & Vaish, R. (2014c). Selection of optimal sintering temperature of $K_{0.5}Na_{0.5}NbO_3$ ceramics for electromechanical applications. *Journal of Asian Ceramic Societies*. 2(1): 5-10.
- [16] Vats, G., Vaish, R., & Bowen, C. R. (2013). Selection of Ferroelectric Ceramics for Transducers and Electrical Energy Storage Devices. *International Journal of Applied Ceramic Technology*.
- [17] Vats, S., Vats, G., Vaish, R., & Kumar, V. (2014). Selection of optimal electronic toll collection system for India: A subjective-fuzzy decision making approach. *Applied Soft Computing*, 21(0), 444-452.
- [18] Saaty, T. L. (1990). How to make a decision: the analytic hierarchy process. *European Journal of Operational Research*, 48(1), 9-26.
- [19] Rao, R. V. (2006). A material selection model using graph theory and matrix approach. *Materials Science and Engineering: A*, 431(1), 248-255.
- [20] Azimi, M., Taghizadeh, H., Farahmand, N., & Pourmahmoud, J. (2014). Selection of industrial robots using the Polygons area method. *International Journal of Industrial Engineering Computations*, 5(4), 631-646.
- [21] Deng H, Y. C., Willis RJ. (2000). Inter-company comparison using TOPSIS with objective weights. *Comput Oper Res* 27, 963-973.
- [22] Opricovic, S., & Tzeng, G.-H. (2004). Compromise solution by MCDM methods: A comparative analysis of VIKOR and TOPSIS. *European Journal of Operational Research*, 156(2), 445-455.
- [23] Azar, A., Olfat, L., Khosravani, F., & Jalali, R. (2011). A BSC method for supplier selection strategy using TOPSIS and VIKOR: A case study of part maker industry. *Management Science Letters*, 1(4), 559-568.
- [24] Sanayei, A., Farid Mousavi, S., & Yazdankhah, A. (2010). Group decision making process for supplier selection with VIKOR under fuzzy environment. *Expert Systems with Applications*, 37(1), 24-30.
- [25] Shanian, A., & Savadogo, O. (2006). TOPSIS multiple-criteria decision support analysis for material selection of metallic bipolar plates for polymer electrolyte fuel cell. *Journal of Power Sources*, 159(2), 1095-1104.
- [26] Shemshadi, A., Shirazi, H., Toreihi, M., & Tarokh, M. J. (2011). A fuzzy VIKOR method for supplier selection based on entropy measure for objective weighting. *Expert Systems with Applications*, 38(10), 12160-12167.
- [27] Ayağ, Z., & Özdemir, R. G. (2006). A fuzzy AHP approach to evaluating machine tool alternatives. *Journal of Intelligent Manufacturing*, 17(2), 179-190.
- [28] San Cristóbal, J. (2011). Multi-criteria decision-making in the selection of a renewable energy project in Spain: The VIKOR method. *Renewable energy*, 36(2), 498-502.
- [29] Peide, L., & Minghe, W. (2011). An extended VIKOR method for multiple attribute group decision making based on generalized interval-valued trapezoidal fuzzy numbers. *Scientific Research and Essays*, 6(4), 765-776.
- [30] Lai, Y.-J., T.-Y. Liu, and C.-L. Hwang, TOPSIS for MODM. *European Journal of Operational Research*, 199.76(3): 486-500.
- [31] Wang, Y.-M. and T.M.S. Elhag, Fuzzy TOPSIS method based on alpha level sets with an application to bridge risk assessment. *Expert Systems with Applications*, 2006.31(2): 309-319.
- [32] Jahanshahloo, G.R., F.H. Lotfi, and M. Izadikhah, Extension of the TOPSIS method for decision-making problems with fuzzy data. *Applied Mathematics and Computation*, 2006.181(2): 1544-1551.
- [33] Heydar Maddah , Reza Aghayari , Mojtaba Mirzaee, Mohammad Hossein Ahmadi, Milad Sadeghzadeh , Ali J. Chamkha, Factorial experimental design for the thermal performance of a double pipe heat exchanger using $Al_2O_3-TiO_2$ hybrid nanofluid. *International Communications in Heat and Mass Transfer*, 2018. 97: 92-102.
- [34] Milad Sadeghzadeh, Mohammad Hossein Ahmadi, Mostafa Kahani, Hossein Sakhaeinia, Hossein Chaji, Smart modeling by using artificial intelligent techniques on thermal performance of flat-plate solar collector using nanofluid. *Energy Science and Engineering*, 2019, doi.org/10.1002/ese3.381.